LOW-FIELD NUCLEAR MAGNETIC RESONANCE CHARACTERIZATION OF ORGANIC CONTENT IN SHALES

Kathryn E. Washburn[1], Justin E. Birdwell[2], Joseph D. Seymour[3], Catherine Kirkland[3], Sarah J. Vogt[3,4]

1. Weatherford Laboratories, 8845 Fallbrook Drive, Houston TX, 77064
2. U.S. Geological Survey, Denver Federal Center, Box 25406 MS 977, Denver CO 80225
3. Chemical and Biological Engineering, Montana State University, 306 Cobleigh Hall, Bozeman MT 59717
4. Department of Chemical and Mechanical Engineering, University of Western Australia

This paper was prepared for presentation at the International Symposium of the Society of Core Analysts held in Napa Valley, California,, USA, 16-19 September, 2013.

ABSTRACT

Low-field nuclear magnetic resonance (LF-NMR) relaxometry is a non-invasive technique commonly used to assess hydrogen-bearing fluids in petroleum reservoir rocks. Longitudinal T_1 and transverse T_2 relaxation time measurements made using LF-NMR on conventional reservoir systems provides information on rock porosity, pore size distributions, and fluid types and saturations in some cases. Recent improvements in LF-NMR instrument electronics have made it possible to apply these methods to assess highly viscous and even solid organic phases within reservoir rocks. T_1 and T_2 relaxation responses behave very differently in solids and liquids, therefore the relationship between these two modes of relaxation can be used to differentiate organic phases in rock samples or to characterize extracted organic materials. Using T_1-T_2 correlation data, organic components present in shales, such as kerogen and bitumen, can be examined in laboratory relaxometry measurements. In addition, implementation of a solid-echo pulse sequence to refocus some types of T_2 relaxation during correlation measurements allows for improved resolution of solid phase protons.

LF-NMR measurements of T_1 and T_2 relaxation time correlations were carried out on raw oil shale samples from resources around the world. These shales vary widely in mineralogy, total organic carbon (TOC) content and kerogen type. NMR results were correlated with Leco TOC and geochemical data obtained from Rock-Eval. There is excellent correlation between NMR data and programmed pyrolysis parameters, particularly TOC and S2, and predictive capability is also good. To better understand the NMR response, the 2D NMR spectra were compared to similar NMR measurements made using high-field (HF) NMR equipment.

INTRODUCTION

Nuclear magnetic resonance is a commonly used method in the petroleum industry to assess porosity, pore size distributions, and fluid types [1]. It has the advantage over other techniques, particularly other wireline measurements, of being lithology independent in conventional reservoirs. An NMR measurement is taken by applying a strong magnetic field to a system. The magnetic moments of nuclei line up along the applied magnetic field. Radio frequency pulses are applied to the system to excite the magnetic moment of hydrogen nuclei away from the applied magnetic field. After the system is excited, the NMR signal returns to equilibrium via two different, simultaneous mechanisms. The first, longitudinal T_1 relaxation, is the time it takes for the excited magnetization to return to equilibrium along the applied magnetic field. The second is transverse T_2 relaxation, which is the time it takes for the spins to come to equilibrium among themselves, going from a highly ordered state to a completely disordered state. By observing these two relaxation mechanisms, we can gain information regarding the porous system and the saturating fluids.

Recently, there has been an increased focus in the industry upon unconventional resources. While some unconventional resources contain significant quantities of hydrocarbons, they often have extremely low permeability. This makes evaluation of these samples via standard core analysis methods difficult, as flow of liquids or gases through samples is difficult or impossible [2,3]. Because NMR is non-invasive, it is a method that has gained significant attention for characterization of unconventional resources such as shales, but additional challenges arise when performing NMR on these samples. For conventional reservoirs, most of the hydrogen atoms are associated with fluid within pores; there is typically little hydrogen in the matrix itself. As a result, the measured relaxation times are assumed to be a reflection of the underlying pore size distribution, described by the relation [4]:

$$\frac{1}{T_{1,2}} = \frac{1}{T_{1,2Bulk}} + \rho_{1,2}\frac{S}{V}$$

where $T_{1,2Bulk}$ is the bulk relaxation times for T_1 and T_2 respectively, $\rho_{1,2}$is the surface relaxivity, S is the pore surface area and V is the pore volume. Small pores have a high surface-area-to-volume ratio and relax quickly while larger pores have a smaller surface-area-to-volume ratio and relax more slowly. However, in unconventional reservoirs, there may be significant quantities of hydrogen present in organic materials such as kerogen and bitumen. The relaxation behavior of viscous solids and semi-solids such as these deviates from the conventional behavior of low viscosity liquids in porous materials. Instead of interactions with the pore surfaces controlling the relaxation rate, the relaxation is heavily influenced or dominated by intramolecular dipolar coupling within the solid or semi-solid. This relaxation behavior is described by the following equations [5]

for T_1;

$$\frac{1}{T_1} = \left(\frac{6}{20}\right) \times \left(\frac{\hbar^2 \gamma_I^2 \gamma_S^2}{r^6}\right) \times \left(\frac{\tau_c}{1 + \omega_0^2 \tau_c^2} + \frac{4\tau_c}{1 + 4\omega_0^2 \tau_c^2}\right)$$

and for T_2;

$$\frac{1}{T_2} = \left(\frac{3}{20}\right) \times \left(\frac{\hbar^2 \gamma_I^2 \gamma_S^2}{r^6}\right) \times \left(3\tau_c + \frac{5\tau_c}{1 + \omega_0^2 \tau_c^2} + \frac{2\tau_c}{1 + 4\omega_0^2 \tau_c^2}\right)$$

where, γ_I and γ_S are the gyromagnetic ratio of the interacting nuclei, $\hbar$ is Planks constant over 2π, r is the distance between interacting nuclear, $\omega_0$is the resonance frequency of the system and τ_c is the correlation time.

For low viscosity fluids, the molecules are able to tumble freely and τ_c is very short, giving long relaxation times and similar values of T_1 and T_2. In this situation, for a fluid filled porous material in the fast diffusion limit [6], the effect of intramolecular dipolar coupling is small compared to the effects of surface relaxivity, and traditional interpretation of fluid filled porous materials can be applied. For highly viscous or solid materials, molecular motion is highly restricted so that the correlation time of the fluid is long and, T_1 will be longer than T_2. For porous materials containing these types of fluids, the sample relaxation behaviour is strongly influenced by their intramolecular dipolar coupling. We make use of this distinct difference in relaxation ratios by running T_1-T_2 correlation measurements [7] in order to separate out sample constituents with differing viscosities. Fluid-like constituents will be close to T_1-T_2 parity while the more viscous and solid constituents will have T_1 and T_2 values that differ significantly [5].

In addition, a recent study has shown that a significant amount of transverse relaxation in organic rich systems may arise from homonuclear dipolar coupling [8]. Standard T_1 and T_2 techniques will not recover signal lost from this type of interaction. A conventional T_1-T_2 correlation measurement, shown in Figure 1a, uses a spin-echo train [9,10], a series of 180° pulses, to measure T_2. This type of pulse sequence will only refocus dephasing caused by heteronuclear dipolar coupling. To recover the additional magnetization dephasing caused by homonuclear dipolar coupling, we also apply a solid-echo T_1-T_2 correlation technique, Figure 1b. The solid-echo method applies a series of 90° pulses, instead of a series of spin echoes to measure T_2.

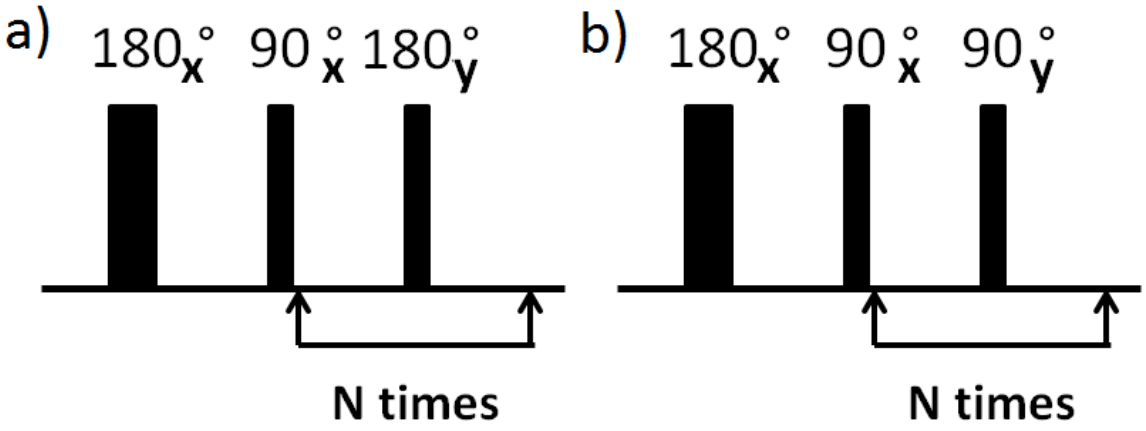

Figure 1. a) T_1-T_2 Spin-echo Pulse Sequence b) T_1-T_2 Solid-echo Pulse Sequence

Some concerns arose about the results given the extremely short nature of the relaxation times. It was unclear if at low field a full description of relaxation for all sample constituents was being obtained. To address this, several samples were run at high-field, with a shorter echo spacing to attempt to gain a more complete assessment of the relaxation distributions in the samples. It is anticipated from theory that the T_1 values of the samples would increase, but given that the majority of T_2 relaxation arises from homonuclear dipolar coupling, it was expected that there would be less influence of the increased magnetic field on the T_2 distributions.

To further interpret the NMR results, the data were correlated to geochemical parameters determined by Rock-Eval programmed pyrolysis and LECO total organic carbon (TOC) analyses [11,12]. Programmed pyrolysis gives information related to the content of bitumen (S1), kerogen (S2), and kerogen-derived carbon dioxide (S3). A partial least squares regression (PLSR) analysis [13] was used to perform the correlation between the NMR results and the programmed pyrolysis and TOC values. PLSR is a multivariate method for correlating the greatest amounts of variance in a dataset with the greatest amount of variance in the values to be predicted and is widely used to predict difficult to measure chemical parameters from spectroscopic data in a variety of industries.

METHODS:

The work for this study was performed on oil shales, which are frequently confused with other types of petroleum resources. Oil shales are immature source rocks containing significant quantities of organic matter that have not undergone catagenesis to produce oil, gas, or significant amounts of bitumen. They contain kerogen and small amounts of naturally occurring bitumen, but no liquid hydrocarbons. The amount of kerogen can range up from trace amounts to 70% by volume in the richest oil shales. This makes them a useful starting case for characterization of organic solids, without the complexity of assessing both liquid and solid organic components.

The 18 oil shales included in this study represent a range of materials from deposits around the world. We focus on a subset of four of these shales for discussion of the NMR results: Ordovician Narva-E kukersite (Estonia); Permian Glen Davis torbanite (Australia); Cretaceous Timahdit marinite (Morocco); and Cambrian Alum marinite (Sweden). All samples were crushed to a uniform size (~2 mm) but otherwise were unaltered.

Rock-Eval analysis and TOC content measurements were conducted by Weatherford International at the Shenandoah, Texas laboratory using a Rock-Eval 2 instrument (Delsi Inc., Houston, TX) and standard operating parameters for programmed pyrolysis (Peters, 1986; Behar et al., 2001; McCarthy et al., 2011) and using a LECO C230 TOC analyzer (LECO Corporation, St. Joseph, MI) following the manufacturer's instructions. Qualitative assessment of sample mineralogy was obtained from Fourier transform infrared measurements on raw and low temperature ashed samples using a Bruker ALPHA spectrometer (model A250/D, Bruker Optics, Inc., Billerica, MA) equipped with an attenuated total reflectance sampling module (model A220/D-01) and a diamond internal reflection element.

LF-NMR measurements were performed using a 2 MHz Magritek Rock core analyser equipped with a 35 mm probe optimized for shale results. For the LF-NMR measurements, the crushed samples were placed in 1 inch diameter test tubes, which were filled to a height of 2 inches. This corresponds to the maximum sample volume for the probe. All echoes were performed with a 30 μs τ value, the minimum value possible with this equipment. Two thousand echoes were measured for both the spin-echo and solid-echo measurements. For T_1, 40 logarithmically spaced points were measured from 0.03 ms to 3000 ms. The T_1-T_2 correlation results were inverted using a maximum entropy method [14] to create a 40 by 40 matrix. Previous work indicates the inversion is stable and accurately calculates the signal intensity over the range of relaxation times [8].

HF-NMR measurements were performed using a 300 MHz Bruker equipped with a 5 mm imaging probe networked to an AVANCE III spectrometer. For the HF-NMR measurements, the crushed samples were placed in a 5 mm NMR test tube and filled to a height of approximately 2 inches, which completely fills the active measurement volume of the probe. Measurements were performed with a 11 μs τ value and 3000 echoes. T_1 was measured with 32 logarithmically spaced points from 1 ms to 50s. Only the spin-echo measurements were performed at high-field.

Multivariate data analysis was performed using the commercial software package The Unscrambler® version 10.2 (CAMO Software AS, Oslo, Norway) with the standard Partial Least Squares package. No sample specific signal processing was performed on the results. The spectra were transformed from a 2D matrix to a 1D vector prior to analysis and the log of the intensities taken before regression, which makes the analysis less sensitive to minor peak shifts. Cross-validation was performed using the "leave one out" method. Cross-validation is an important quality control step to ensure that over-

fitting, where the model fits very well to existing data but fails to predict new data, has not occurred.

RESULTS:

NMR, TOC, and geochemistry measurements were performed on a set of 18 oil shales from around the world. We focus on a subset of four, the Estonian Kukersite, Glen Davis, Timadiht and Alum shales, for discussion. The TOC and geochemical properties of these shales are presented in Table 1. The Estonian kukersite is a carbonate-rich shale with significant quantities of clay and quartz containing what has been described as an intermediate kerogen type (II/I). The Glen Davis torbanite was quartz and clay-rich and contains significant quantities of type I kerogen. The Timahdit shale was clay-rich, with significant quantities of feldspars and quartz as well as some carbonate and an intermediate kerogen type (I/II). The Alum shale was made up predominantly of quartz and clay and contained type II kerogen.

	TOC (wt. %)	S1(mg-hydrocarbons/g-rock)	S2 (mg-HC/g-rock)	S3(mg-CO_2/g-rock)
Alum	12.5	0.7	57.4	2.6
Glen Davis	56.2	3.7	521.5	3.0
Kukersite	44.7	0.4	439.2	5.6
Timadiht	9.5	1.1	53.1	2.4

Table 1. Summary of geochemical parameters.

The LF-NMR T_1-T_2 spin-echo correlation experiments are shown for the subset of samples in the top panels of Figure 2. The corresponding T_1-T_2 solid-echo correlation LF-NMR measurements for the samples are shown in the bottom panel of Figure 2. The LF-NMR samples display the majority of their signal well away from the T_1-T_2 parity line, with short T_2 and long T_1 relaxation times. This is as expected, given the majority of hydrogen in these samples either resides in kerogen or water associated with minerals. For the Alum and Timahdit samples, there is a significant peak at approximately $T_1 = 3\times10^{-4}$, $T_2 = 1\times10^{-4}$ seconds. This peak appears to be significantly weaker in the results for the kukersite and Glen Davis samples. Previous work suggests this peak may be associated with water trapped in interlayer potassium sites in illite [8]. Both the Timahdit and Alum samples are clay-rich, so this interpretation is in agreement with our results. Although the Glen Davis and Kukersite samples also contain clay minerals, the peak associated with the clays is significantly weaker for the two samples. This may be an artifact due to the stronger, dominant peaks nearby affecting the signal intensity. Alternatively, the clays may be less hydrated due to the specific mineralogy or sample handling.

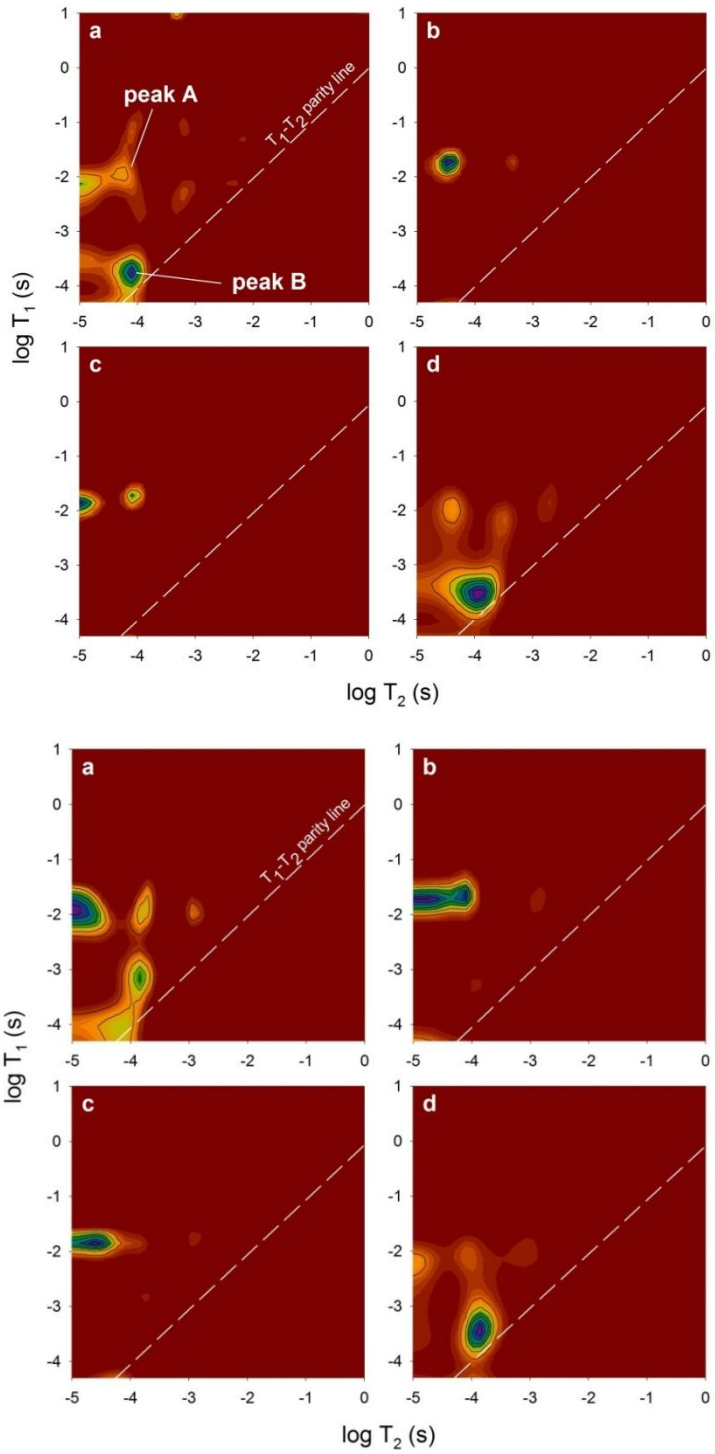

Figure 2. T_1-T_2 Spin-echo (top panels) and T_1-T_2 Solid-echo correlations (bottom panels) for a) Alum b) Glen Davis c) Kukersite d) Timahdit shales.

The HF-NMR results, Figure 3, show relaxation times with significantly longer T_1 values than was observed in the low-field data, as expected. While the distribution of T_2 times seems similar to the low-field results, the observed signal at very short T_2 values appears to be significantly less in the HF-NMR measurements compared to signal at relatively longer times than in the LF-NMR measurements. Although the signal appears to be more intense at short T_2 times in the HF-NMR results, these signals are just much weaker compared to the strong signals at short times and as such are simply less prominent in the LF-NMR plots. While the dipolar coupling constant is independent of field strength, the effect upon the spectral density function is not field independent. This means it is likely that some of the signal at high-field is relaxing at rates beyond what is measureable even with the short tau of 11 μs. Further studies using specialized equipment for solid materials, which can operate with very short pulse and dead times, will be necessary to clarify the full relaxation dynamics. It is possible that relaxation measurements on low-field systems are able to see more of the hydrogen present in the sample than those operating at higher fields. However, the relaxation regimes of solids at low fields have not been thoroughly studied and therefore this issue requires further testing.

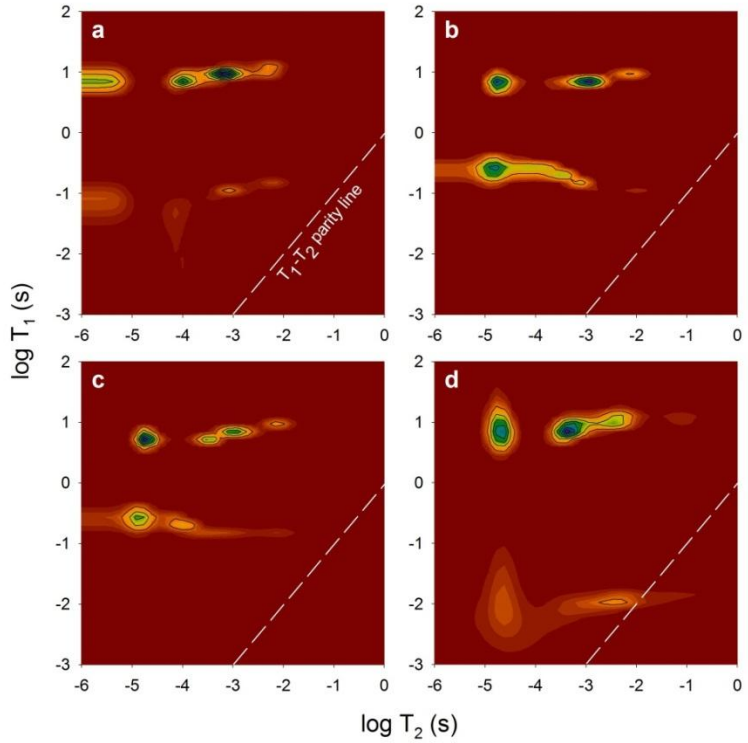

Figure 3. T_1-T_2 spin-echo correlations (HF-NMR) for a) Alum b) Glen Davis c) Kukersite d) Timahdit shales.

The solid-echo measurements show a significant increase in peaks at shorter T_2 for most of the samples. Total signal intensity for each LF-NMR dataset is shown in Table 2. In

addition, two selected peaks, labeled in Figure 2a, were integrated separately. These values are presented in Table 3.

	Spin-echo	Solid-echo
Alum	6.72	7.39
Glen Davis	22.89	78.63
Kukersite	15.17	40.44
Timahdit	12.05	16.75

Table 2. Total signal intensity for spin-echo and solid-echo measurements

	Peak A Spin-echo	Peak A Solid-echo	Peak B Spin-echo	Peak B Solid-echo
Alum	1.08	2.313	3.118	3.527
Glen Davis	19.04	69.13	0.481	1.554
Kukersite	12.38	34.67	0.848	1.388
Timahdit	1.69	2.175	9.028	10.89

Table 3. Peak signal intensity for spin-echo and solid-echo measurements

The signal intensity for Peak A, which we associate with kerogen, increased roughly 2.5 to 3 times in intensity for the Alum, Glen Davis, and kukersite samples using the solid-echo method. The level of increase for the Timahdit was only approximately 50% more than in the spin-echo measurements, which is more in line with previous results. Why the different samples show different increases in signal intensity by spin- and solid-echo methods is uncertain and requires further analysis to elucidate. The solid-echo is only able to completely refocus dephasing due to isolated spin pairs and will be less efficient at refocusing the magnetization of a hydrogen atom undergoing multiple homonuclear dipolar interactions. Also, the presence of paramagnetics can decrease signal intensity. As such, it is expected that kerogen type, mineralogy, or other geochemical factors may play a role in the change of signal intensity between spin and solid-echo measurements. Peak B, which we associate with interlayer water, showed only minor increases between the spin and solid-echo measurements. Additional uncertainty may arise in interpretation due to shifting of peaks that occurs between the two types of measurements.

In addition to the basic integration of peak intensity, PLSR was performed to correlate the NMR spin-echo results to geochemical parameters. The results for S1 (not shown) indicate there is a correlation with the spin-echo results, but the predictive capability is limited. As the oil shale samples only contain a small amount of bitumen, these are suboptimal samples for characterizing this phase. We speculate that a larger sample set with a wider range of S1 values will improve predictability.

PLSR models were generated that produced good correlations and predictive capability for TOC and S2 and the results are shown in Figure 4 (left-side panels). Each parameter

was correlated and predicted using its own model. The blue squares are the correlation results and the red circles are the cross validation predictions. The model to predict TOC from the NMR results produced an excellent correlation and very good predictive capability with R^2 values of 0.993 and 0.876, respectively. An R^2 of 0.9 is the usual maximum expected for predictive capability with samples not run on the exact same material. The PLSR model for S2 also produced excellent correlations and predictive capabilities, with R^2 values of 0.994 and 0.843, respectively. An S3 model was also attempted, but overall the results were poor (not shown), which is not unexpected, as the parameter is associated with oxygen and the LF-NMR technique used here directly assesses only hydrogen.

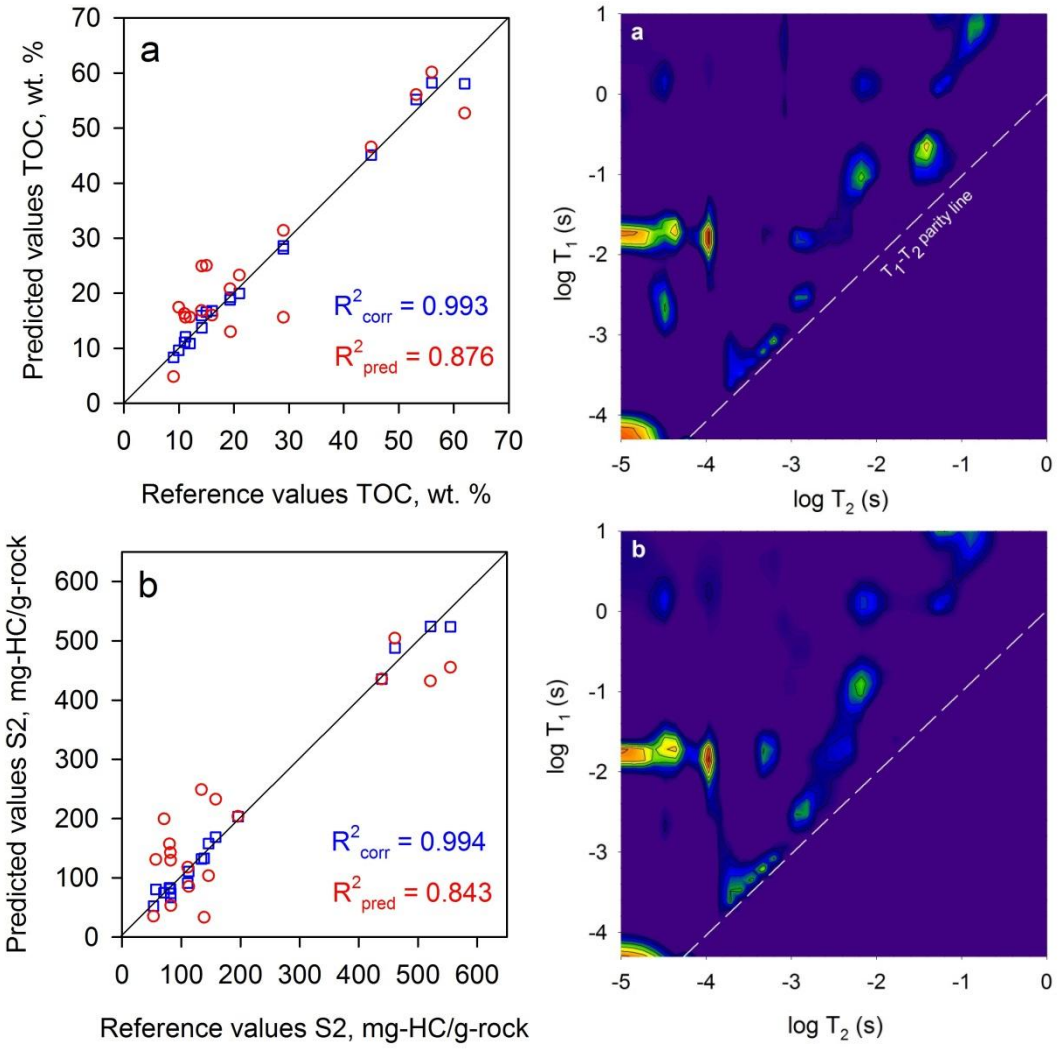

Figure 4. PLSR model predicted versus measured (left panels) and Regression coefficients showing which portions of the NMR spectra are important for prediction of (right panels) a) TOC b) S2

The resulting PLSR correlations only required 5-6 factors to explain the majority of variance in each system, indicating a robust predictive model. Factors are orthogonal linear combinations of the original variables, in this case the 1600 points from the 40 by 40 2D T_1-T_2 correlation matrix, that describe the maximum correlation with the dependent variables. They not only describe the location of the important portions of the spectra, but adjust for non-linearities in the data across the range of prediction. The low number of factors suggests that NMR could be used to predict TOC and S2 in a variety of samples despite differences in mineralogy or kerogen type. The number of factors could be further reduced in the future by limiting prediction to samples of similar mineralogy or organic content, as more factors are necessary to adequately predict within sample sets that are highly heterogeneous. Unfortunately, due to the small sample set, there is not currently enough data to create a test set and check how well the models predict TOC and geochemical quantities for shales that have not been used to develop the predictive model. This is the subject of further work.

To better interpret the NMR T_1-T_2 plots visually, the regression coefficients of the PLSR models were rewrapped into a two dimensional format and displayed. These are shown in Figure 4 (right-side panels). The regression coefficients show which portion of the T_1-T_2 correlation plots are important for the different geochemical parameters. Red indicates areas of strong positive correlation where dark blue indicates areas of negative correlation. We can see that for the S2 parameter, associated with kerogen, that the resulting correlations indicate that that signal around $T_1 = 1\times10^{-2}$ s and $T_2 = 1\times10^{-5}$ to 1×10^{-4} s has the greatest influence on the predicted values. This is in agreement with previous results of LF-NMR measurements upon kerogen and bitumen, which indicated the signal associated with kerogen was located within this range of relaxation times [8]. The resulting regression coefficients for the TOC prediction are extremely similar to those from S2, which is not surprising given that kerogen is the dominant form of organic matter in the oil shales. There also seems to be some weaker correlation with the results from signal around $T_1 = 1\times10^{-1}$ s and $T_2 = 1\times10^{-2}$ s. Whether this is a real effect or an artifact of the small samples size requires further study.

CONCLUSIONS

The combination of T_1-T_2 spin-echo and solid-echo LF-NMR techniques appear to be very promising for providing non-destructive geochemical information on unconventional source rock samples. This would allow for estimation of geochemical parameters for bulk samples, perhaps providing more thorough characterization. In addition, the results presented inform interpretation of what the results of NMR measurements on shale samples mean. The use of PLSR shows potential for producing predictive models that can provide TOC and S2 with a high degree of accuracy. However, the data sample size presented here is limited. Further work upon a wider range of naturally matured shales containing a range of organic and mineralogical constituents is needed for increased characterization of the robustness of the technique. In addition, work needs to be performed on fluid-bearing organic shales to take into

account the complexities that may be introduced due to interactions between solid and liquid constituents in the samples.

ACKNOWLEDGEMENTS

The authors thank Michael Lewan, Jeremy Boak, Alan Burnham and Jack Dyni for help with sample procurement and Max Goldstein for assistance in sample running. Any use of trade, product or firm names is for descriptive purposes only and does not imply endorsement by the U.S. Government.

REFERENCES

1. G. Coates, L. Xiao, M. Prammer *NMR Logging and Principles* Halliburton Energy Services (1999)
2. D. Luffel, F. Guidry, *New core analysis methods for measuring reservoir rock properties of Devonian shale*, J. Pet. Tech. 44 (1992) 1184-1190.
3. R. Loucks, R. Reed, S. Ruppel, D. Jarvie, *Morphology, genesis, and distribution of nanometer scale pores in silicious mudstones of the Mississippian Barnett shale*, J. Sedi. Res. 79 (2009) 848-861.
4. R. Kleinberg, W. Kenyon, P. Mitra, *Mechanism of NMR relaxation of fluids in rock*, J. Magn. Reson 103 (1994) 206-214.
5. N. Bloembergen, E.M.Purcel, R.V.Pound, *Relaxation effects in nuclear magnetic resonance absorption*, Phys. Rev. 73 (1948) 679-712.
6. K. Brownstein, C. Tarr, *Spin lattice relaxation in a system governed by diffusion*, Trans. AIME 26 (1977) 17-24
7. Y.Q. Song, L. Venkataramanan, M. Hurlimann, M. Flaum, P. Frulla, C. Straley *T1-T2 Correlation Spectra Obtained Using a Fast Two-Dimensional Laplace Inversion* J. Magn. Reson 154 (2002) 261-268
8. K.E. Washburn, J.E. Birdwell *Updated Methodology for Nuclear Magnetic Resonance Characterization of Shales* J. Magn Reson 223, (2013) 17-28
9. H. Carr, R. Purcell, *Effects of diffusion on free precession in nuclear magnetic resonance experiments*, Phys. Rev. 94 (1954) 630-638.
10. S. Meiboom, D. Gill, *Aging and non-linear rheology in suspensions of peo-protected silica particles*, Rev. Sci. 29 (1958) 688.
11. B. Tissot, D. Welte, *Petroleum Formation and Occurrence*, Springer Verlag, Berlin, (1984)
12. M. Bordenave, *Applied Petroleum Geochemistry*, Editions Technip, Paris,(1993)
13. H. Martens, T Næs. *Multivariate Calibration*, John Wiley & Sons, Chichester (1992)
14. E. Chouzenoux, S. Moussaoui, J. Idier, F. Mariette, *Efficient maximum entropy reconstruction of nuclear magnetic resonance T1-T2 spectra*, IEEE Trans. On Sign. Proc. 58 (2010) 6040-6051